Low Complexity Linear Detectors for Massive MIMO with Several Antenna Array Configurations: A Comparative Study

Mohammed Elhefnawy[1] and Mahmoud A. Albreem[2]
[1] Department of Electrical Engineering, October 6 University, October 6, Egypt
[2] Department of Electrical Engineering, University of Sharjah, Sharjah 27272, UAE
Email: mmmelhefnawy.eng@o6u.edu.eg; malbreem@sharjah.ac.ae

***Abstract*—In Multiple-Input Multiple-Output (MIMO), there is multi-user interference because of the limited number of antennas at the Base Station (BS). Deploying more antenna elements at the BS to decrease the multi-user interference is a costly solution. Therefore, changing the configuration of antenna arrays at the BS is implemented as an alternative. In this paper, the impact of BS antenna array configurations on the performance of massive MIMO detection techniques is investigated where four different antenna array configurations are implemented at the BS: Uniform Linear Array (ULA), Uniform Rectangular Planar Array (URPA), Uniform Circular Array (UCA) and Uniform Circular Planar Array (UCPA). The performance of the massive MIMO system is based on the millimeter wave (mmWave) channel that depends on the array response vector of the BS antenna array configuration. To the best of our knowledge, this is the first paper to investigate the impact of antenna array configurations at the BS on the performance and the computational complexity of massive MIMO detection techniques. Numerical results show that the implementation of URPA at the BS with MMSE detection algorithm can achieve the best performance of BER=10^{-4} at SNR = 9dB. The deployment of the UCA at the BS with the successive over-relaxation (SOR), the Gauss-Seidel (GS), and the conjugate-gradient (CG) detection methods provides a performance of BER=10^{-4} at SNR = 12dB when the number of iterations equals eight. In the case of using the UCA at BS with the Richardson (RI) detection method, the number of iterations is required to be increased to achieve the same performance. To achieve BER=10^{-4}, the detector based on the CG method has the lowest computational complexity while the RI method has the highest complexity.**

***Index Terms*—Massive MIMO, detection, antenna array configurations, Fifth-Generation, computational complexity**

I. Introduction

It is foreseeable that efficient technologies are playing a crucial role in Fifth-Generation (5G) and Beyond 5G (B5G) to achieve the user demands in both the performance and the Quality of Services (QoS). In the millimeter-wave (mmWave), the spectrum from 30GHz to 300GHz is utilized to provide large bandwidth, and thus, the data rate increases up to multi Gigabits per second. The conventional small-scale MIMO technology had been deployed since the Third-Generation (3G) wireless networks to improve the performance of wireless transceivers. Massive MIMO is an extension of the small-scale MIMO and it is a promising candidate to achieve a high data rate, low latency, high energy, and spectral efficiencies. In massive MIMO, a large number of antennas are deployed at the BS to serve a large number of mobile user terminals at the same frequency band where the number of mobile user terminals is noticeably smaller than the number of Base Station (BS) antennas. The increase in the number of antenna elements at the BS requires the use of mmWave to reduce the operating wavelength and pack more antenna elements in a smaller physical space. But as the operating wavelength is decreasing, the carrier frequency is increasing, and the power loss is increasing as well. To compensate for this additional attenuation, higher gain antennas are required to be implemented with the massive MIMO system. If the BS has an unlimited number of antenna elements in a massive MIMO system, the multi-user interference will be eliminated and the mutual orthogonality among the channel vectors of the user's terminals occurs. However, practically there is multi-user interference because of the limited number of antennas at the BS. Deploying more antenna elements at the BS to decrease the multi-user interference is a costly solution so changing the configuration of antenna arrays at the BS is implemented as an alternative [1]-[4].

In literature, a plethora of massive MIMO detectors' structures is proposed to obtain a convenient balance between performance and complexity. Nonlinear detectors are not competitive in realization because they require a decomposition, i.e., QR, LDL, or Cholesky decompositions, which increases the complexity. Detectors based on linear methods are relatively simple and easy to implement but they suffer from a remarkable performance deterioration in highly correlated channel elements. Moreover, they also contain an undesirable matrix inverse which is not easy to implement. To achieve a pleasant balance between the performance and

Manuscript received February 13, 2022; revised April 3, 2022; accepted May 11, 2022.

Corresponding author: Mohammed Elhefnawy (email: mmmelhefnawy.eng@o6u.edu.eg).

doi: 10.18178/ijeetc.11.6.410-418

the complexity of linear massive MIMO uplink detectors, two scenarios are proposed to obtain a free-matrix-inversion detector. These scenarios are well-known among the Very-Large-Scale Integration (VLSI) signal processing community because of their low complexity. The first scenario, such as the Neumann Series (NS) and Newton Iteration (NI) methods, is approaching the matrix inverse instead of exact computation. However, the complexity of the NS method is comparable to the exact matrix inversion algorithm when the expansion order is more than two. In the NI method, matrix multiplications are involved which increases the computational complexity. The second scenario depends on avoiding the matrix inversion by exploiting the iterative methods to solve the linear equations. The Successive Over-Relaxation (SOR), the Gauss-Seidel (GS), the Jacobi (JA), the Richardson (RI), and the Conjugate Gradient (CG) methods are examples of such iterative methods where matrix multiplications are replaced by matrix-vector products. Therefore, solving linear equations with iterative methods is less computational complexity compared with the first scheme. In addition, the first scenario suffers from a slow convergence rate when the number of BS antennas is relatively close to the number of user terminal antennas [5].

In [5] and [6], the fundamentals of data detection techniques were comprehensively presented. The authors have provided an extensive overview of milestones of optimal massive MIMO detection development. The impact of channel effects, precoding, and channel estimation methods are also presented. In [7], the pros and cons of iterative methods were listed where the number of computations and Bit-Error-Rate (BER) are considered. In addition, it is shown that detectors based on RI, OCD, and CG methods can achieve a high Hardware Efficiency (HE) while a detector based on JA has achieved the worst HE. The relaxation parameter effects in RI and SOR methods are also studied. Although [5]-[7] were comprehensive, the impact of antenna array configurations is not well-investigated. In [8], it is shown that linear detectors based on iterative methods could achieve a high-performance enhancement with a low computational complexity when a stair matrix is exploited instead of a diagonal matrix. The article in [9] provides insights on data detection algorithms for decentralized and cell-free massive MIMO. However, the effect of antenna array configurations at the BS is not yet investigated. Therefore, there is still room for fundamental research in data detection for massive MIMO.

The effect of the antenna array configuration at the BS on the performance of MIMO systems was studied in many works of literature. In [3], the inter-element spacing in a ULA at the BS was utilized to decrease the multi-user interference and enhance the performance of the MU-MIMO system. In [4], a rectangular antenna array with non-uniform distances between its elements was implemented at the BS to improve the performance of the FD-MIMO system. In [10], the elements of the antenna array at the BS were divided into multiple sub-arrays antenna configurations, each of which is connected with a single RF chain. The effect of implementing different sub-ULA configurations with the BS on the performance of a massive MIMO system was studied. In [11], the achievable sum rate for the massive MIMO system was investigated, where three different antenna array configurations including ULA, UCA, and URPA were implemented with the BS. The influence of using ULA, URPA, and UCA at the BS on the performance of a massive MIMO system was investigated in [12], where the orthogonality between the channels vectors associated with different users is affected by the antenna array configuration at the BS. In [13], hybrid precoding for millimeter mmWave massive MIMO systems with different antenna configurations has been considered. The spectral efficiency and energy efficiency have been illustrated when ULA, URPA, and UCPA are utilized. However, this paper did not consider the detection scheme and the receiver design.

To the best of our knowledge, this is the first paper to investigate the effect of the antenna array configurations at the BS on the performance and the computational complexity of massive MIMO detection techniques.

This paper is organized as follows: Section II describes the massive MIMO system model. Section III describes the iterative methods to avoid direct computation of matrix inverse. The computational complexity of each method is illustrated in Section IV. Section V presents the antenna array configurations at the BS. Section VI provides the numerical results and Section VII concludes the paper.

II. System Model

In this section, the massive MIMO system model is presented. It is assumed that massive multiuser Base Station (BS) antennas N_r are serving K single-antenna users where $K<<N_r$. The separation between these single-antenna user's devices is many wavelengths so the collaboration between these single-antenna user's terminals does not exist. For the uplink communication scenario, a single-cell massive MIMO system is assumed. The received signal for a time-invariant wireless channel can be expressed as

$$\mathbf{y} = \mathbf{H}\mathbf{x} + \mathbf{n}' \tag{1}$$

The received signal at the BS is $\mathbf{y} \in \mathbb{C}^{N_r \times 1}$, the signals which are transmitted by the user's terminals are represented by a random vector $\mathbf{x} = \left[x_1\, x_2 \cdots x_K\right]^T$, where $\mathbf{x} \in \mathbb{C}^{K\times 1}$, the AWGN random vector is realized by $\mathbf{n}'$, where $\mathbf{n}' \in \mathbb{C}^{N_r \times 1}$, and $\mathbf{H} \in \mathbb{C}^{N_r \times K}$ is the wireless channel matrix between N_r BS and K users. Each mobile device is restricted to have unitary power, so that $E\left[|x_k|^2\right] = 1,\ \forall k \in \{1,\ 2,\ \cdots,\ K\}$, where $E[\cdot]$ denotes the expected value. The mmWave channel of the massive MIMO system is described as [1]

$$\mathbf{H} = \sqrt{\frac{N_t N_r}{N_C N_{\text{ray}}}} \sum_{i=1}^{N_{\text{cl}}} \sum_{l=1}^{N_{\text{ray}}} \alpha_{il}\, \mathbf{a}_r\left(\varphi_{il}^r, \theta_{il}^r\right) \mathbf{a}_t\left(\varphi_{il}^t, \theta_{il}^t\right)^{\mathrm{H}} \tag{2}$$

where $(\cdot)^{\mathrm{H}}$ denotes the Hermitian operators, N_{cl} is the number of scattering clusters, and each cluster has several propagation paths that equal N_{ray}. α_{il} is the gain of each propagation path that follows a complex Gaussian distribution with a variance of $\sigma_{\alpha_i}^2$ and zero mean. The array response vector of the transmitter is represented by $\mathbf{a}_t(\varphi_{il}^t, \theta_{il}^t)$ which is assumed to be independent and identically distributed random variables with unit variance and zero mean, while $\mathbf{a}_r(\varphi_{il}^r, \theta_{il}^r)$ is the array response vector of the receiver. φ_{il}^r and θ_{il}^r are the azimuth and elevation Angles of Arrivals (AoA), respectively; while φ_{il}^t and θ_{il}^t are azimuth and elevation Angles of Departures (AoD), respectively. The angles of arrivals and departures follow the Laplacian random distribution. Each propagation path can be described by three parameters: the complex gains on each path, the AoA of the path at the base station, and the AoD of the path at the mobile terminal. This system model is usually utilized to derive a detection scheme where $\mathbf{x}$ is determined based on the received vector $\mathbf{y}$. It is noteworthy that the channel state information (CSI) at the BS is assumed to be known. In the maximum likelihood (ML) detector, an exhaustive search is conducted where the estimated signal $\hat{\mathbf{x}}$ is illustrated as

$$\hat{\mathbf{x}} = \arg\min \|\mathbf{y} - \mathbf{H}\mathbf{x}\|_2^2 \tag{3}$$

It is worth mentioning that the ML detector is barred in realization because of its extremely high complexity. In a rich scattering environment with a small number of user terminals, a detector based on the matched filter (MF) achieves a good performance where the estimated signal is given as

$$\hat{\mathbf{x}}_{\mathrm{MF}} = \mathbf{H}^H \mathbf{y} \tag{4}$$

In spatially correlated channels, advanced detectors are needed to attain an interesting tradeoff between performance and complexity. Other linear detectors, such as the Zero-Forcing (ZF) and Minimum Mean Square Estimation (MMSE), are alternative low complexity solutions. In the ZF detector, the estimated signal $\hat{\mathbf{x}}$) is illustrated as

$$\hat{\mathbf{x}} = \left(\mathbf{H}^{\mathrm{H}}\mathbf{H}\right)^{-1}\mathbf{H}^{\mathrm{H}}\mathbf{y} = \mathbf{A}_{\mathrm{ZF}}^{\mathrm{H}}\mathbf{y} \tag{5}$$

where $\mathbf{A}_{\mathrm{ZF}}^{\mathrm{H}}$ is the equalization matrix in the ZF detector. It is well known that the effect of noise is neglected in the ZF detector which produces a noise enhancement in the case of small-valued coefficients. The MMSE detector could be implemented to overcome the weakness in the ZF detector. The estimated signal in the MMSE detector is given as

$$\hat{\mathbf{x}} = \left(\mathbf{H}^{\mathrm{H}}\mathbf{H} + \sigma^2\mathbf{I}\right)^{-1}\mathbf{H}^{\mathrm{H}}\mathbf{y} = \mathbf{A}_{\mathrm{MMSE}}^{\mathrm{H}}\mathbf{y} \tag{6}$$

where $\mathbf{A}_{\mathrm{MMSE}}^{\mathrm{H}}$ is the equalization matrix in the MMSE detector. σ^2 and $\mathbf{I}$ are the noise variance and the $K\times K$ identity matrix, respectively. As shown in (5) and (6), the matrix inversion is included in the equalization matrix for both the ZF and MMSE detectors. Due to the high complexity of computation of the matrix inversion, several iterative methods have been proposed and they are well-known in detectors design since 2013.

III. Iterative Matrix Inversion Method

Iterative methods date to the late 18th century when Jacobi (JA) and Gauss-Seidel (GS) iterative methods have been proposed. Matrix inversion exhibits a high computational complexity, thus, it is very seldom to use iterative methods for solving small dimension systems because the time required for a satisfactory accuracy could exceed that required indirect techniques to find the exact solutions, such as the Gaussian Elimination (GE) method. For a large system, iterative methods are efficient to approximate the matrix inversion in terms of both storage and computation. As shown in (5) and (6), matrix inversion is wanted to equalize the received signal and is being one of the awful complex mathematical operations in linear and nonlinear massive MIMO detectors. The problem increases as the MIMO size increases. Several methods are proposed to approximate/avoid the computation of an exact matrix inverse, rather than computing it. In addition, a challenge of matrix inversion also lies and the system is characterized as ill-conditioned when the channel matrix is nearly singular. In this situation, advanced detectors are in demand to overcome the inherent noise enhancement. In this section, we present the iterative matrix inversion methods in the context of massive MIMO detectors where the number of iterations and the systems' size are playing a major role in achieving a balance between complexity and performance. The convergence rate of each method has a great impact on achieving a satisfactory balance between performance and complexity. The convergence rate is based on the spectral radius of the associated matrix. It is well known that the spectral radius $\rho(\mathbf{H})$ of a matrix $\mathbf{H}$ is defined by

$$\rho(\mathbf{H}) = \max|\lambda| \tag{7}$$

where λ is an eigenvalue of $\mathbf{H}$. However, ρ(H) is strongly related to the norm of a matrix. One way to choose a procedure to accelerate convergence is to select a method whose associated matrix has minimal ρ(H). The aim is to fully void the matrix inversion of the Gram or Gramian matrix $\mathbf{G}=\mathbf{H}^{\mathrm{H}}\mathbf{H}$. In other words, $\mathbf{G}^{-1}$ will not be calculated or approximated. However, the received signal is equalized through iterative methods such as the GS, the CG, the SOR, the JA, and the RI. As mentioned earlier, the number of iterations and the initial solution are playing a pivotal role in achieving a pleasurable performance-complexity profile.

A. Successive Over Relaxation

The SOR method is a well-known iterative method where the estimated signal is described as

$$\hat{\mathbf{x}}^{(n)} = \left(\frac{1}{\omega}\mathbf{D}+\mathbf{L}\right)^{-1}\left[\hat{\mathbf{x}}_{\mathrm{MF}}+\left[\left(\frac{1}{\omega}-1\right)\mathbf{D}-\mathbf{U}\right]\hat{\mathbf{x}}^{(n-1)}\right] \quad (8)$$

where ω, $\mathbf{D}$, n, $\mathbf{L}$, and $\mathbf{U}$ are the relaxation parameter, diagonal matrix, number of iterations, strictly lower and upper triangular components, respectively [14]. The relaxation parameter (ω) plays a crucial role in the systems' performance-complexity profile. However, the method is called the under-relaxation method if $0<\omega<1$ while it is called the over-relaxation method if $\omega>1$. The profile of a detector is greatly influenced by the initial solution $\hat{\mathbf{x}}^{(0)}$ where the common selection is $\hat{\mathbf{x}}^{(0)} = \mathbf{D}^{-1}\hat{\mathbf{x}}_{\mathrm{MF}}$. If there is no prior knowledge about the initial solution $\hat{\mathbf{x}}^{(0)}$, it can be considered as a zero vector. The main drawback of this detector is an uncertain relaxation parameter since it could be greater than zero and smaller than 2. In addition, **G** has to be pre-computed and supplied as an input to the method which could increase the computational complexity.

B. Gauss-Seidel

The GS method is a distinctive status of the SOR method, where the relaxation parameter is considered as $\omega = 1$. The estimated signal is given as

$$\hat{\mathbf{x}}^{(n)} = \left(\mathbf{D}+\mathbf{L}\right)^{-1}\left(\hat{\mathbf{x}}_{\mathrm{MF}}-\mathbf{U}\hat{\mathbf{x}}^{(n-1)}\right) \quad (9)$$

This method is not appropriate for parallel computation due to the internal sequential iterations structure. However, the GS-based detector requires lower computational complexity than a detector based on the SOR method [15]. Like the SOR method, the initial solution can be considered as $\hat{\mathbf{x}}^{(0)} = \mathbf{D}^{-1}\hat{\mathbf{x}}_{\mathrm{MF}}$. If there is no prior knowledge about $\hat{\mathbf{x}}^{(0)}$, it can be considered a zero vector.

C. Jacobi

The JA method is an iterative method where the diagonal matrix has a great impact to find the estimated signal as

$$\hat{\mathbf{x}}^{(n)} = \mathbf{D}^{-1}\left(\hat{\mathbf{x}}_{\mathrm{MF}}+\left(\mathbf{D}-\mathbf{A}\right)\hat{\mathbf{x}}^{(n-1)}\right) \quad (10)$$

which is applicable if

$$\lim_{n\to\infty}\left(\mathbf{I}-\mathbf{D}^{-1}\mathbf{A}\right)^{n} = 0 \quad (11)$$

A detector that depends on the JA method converges slowly, and therefore, implies high latency [16]. In addition, it is not achieving optimal performance when the ratio of the user terminal to BS antennas is close to one. In general, the computational complexity required by the JA method is lower than the required in the SOR and GS methods. In general, the JA method guarantees that the first iteration is multiplication free and thus, complexity is low.

D. Richardson

The RI method is an iterative method where ω plays a crucial role in the performance-complexity profile [17]. Unlike the SOR, GS, and JA methods, it is executing certain vector operations and multiplications by H where the estimated signal is obtained as

$$\hat{\mathbf{x}}^{(n)} = \hat{\mathbf{x}}^{(n-1)} + \omega\left(\mathbf{y}-\mathbf{H}\hat{\mathbf{x}}^{(n-1)}\right) \quad (12)$$

It is shown that a good enough balance between the computational complexity and the performance can be achieved when $0<\omega<2/\lambda$, where λ is the largest eigenvalue of **H**. Also a high number of iterations is required to converge. However, the RI method is marked as a hardware-friendly method.

E. Conjugate-Gradient

The CG method was originally designed to solve a positive definite linear system [18]. Large sparse systems with nonzero entries occurring in predictable manners could be solved by implementing the CG method. The estimated signal can be obtained as

$$\hat{\mathbf{X}}^{(n)} = \hat{\mathbf{X}}^{(n-1)} + \alpha^{(n-1)} p^{(n-1)} \quad (13)$$

where $p^{(n-1)}$ and $\alpha^{(n-1)}$ are the conjugate direction and a scalar parameter, respectively. A detector based on the CG method achieves a quasi-optimal performance when the ratio between the user terminals and BS antennas is small. A detector based on the CG method could achieve good performance with low complexity as compared with the SOR, GS, JA, and RI methods.

IV. Complexity Analysis

The computation of a matrix inverse requires a large number of divisions and multiplications. The computational complexity of a massive MIMO detector is dominated by matrix multiplications. Table I shows the complexity comparison between different iterative methods based on the number of multiplications.

TABLE I: COMPLEXITY COMPARISON AMONG FREE-MATRIX INVERSION METHODS

Method	Number of Multiplications
SOR	$4nk^2+k(n+3)-3$
GS	$4nk^2+3(k-1)$
RI	$4nk^2+k(2n+3)-3$
CG	$n(N+2k^2)$
JA	$2nk(2k-1)$

V. Base-Station Antenna Array Configurations

The antenna arrays provide higher directivity than that of their antenna element. The antenna array at the BS is generally selected to be uniform. There are various configurations of the uniform antenna arrays which can be implemented with the BS in the mmWave massive MIMO systems. The most common configurations of those antenna arrays include a Uniform Linear Array (ULA), a Uniform Planar Rectangular Array (UPRA), a Uniform Circular Array (UCA), and a Uniform Circular Planar Array (UCPA) [2], [19], [20]. In this paper, these four uniform antenna array configurations are considered to be implemented with the BS. Each antenna array configuration consists of 126 isotropic antenna elements.

A. Uniform Linear Array (ULA)

As shown in Fig. 1, the ULA is a one-dimensional antenna array where the array response vector for the ULA of N_r elements along the x-axis can be expressed as [2]

$$\mathbf{a_r}(\varphi,\theta)_{\text{ULA}} = \sum_{m_x=1}^{N_r} I_{m_x} e^{j(m_x-1)(kd_x \sin\theta\cos\varphi+\beta_x)} \quad (14)$$

All the ULA elements are equispaced with an interval of $d_x = \lambda_o/2$, where φ and θ are the azimuth and elevation angles, respectively, $k = 2\pi/\lambda_o$, λ_o is the free space wavelength of the signal. The applied excitation weights are set to $I_{m_x} = 1$ and the progressive phase shift is set to $\beta_x = 0^\circ$. The length of a ULA is about $62.5\lambda_o$.

B. Uniform Rectangular Planar Array (URPA)

The implementation of the URPA with the BS results in increasing the number of antenna elements within a small area. In x-direction, the number of antenna elements equals M with the separation distance between every two neighboring elements $d_x = \lambda_o/2$. N elements in the y-direction are equispaced at a distance $d_y = \lambda_o/2$. The URPA consists of M×N elements as shown in Fig. 2.

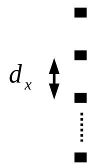

Fig. 1. The configuration of Uniform Linear Array (ULA).

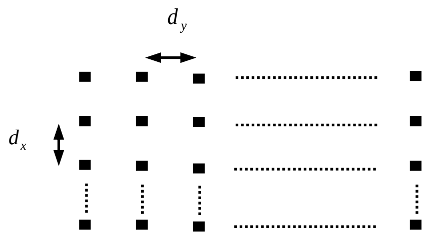

Fig. 2. Configuration of uniform rectangular planar array (URPA).

The array response vector of the URPA can be given by [21]

$$\mathbf{a_r}(\varphi,\theta)_{\text{URPA}} = \sum_{m_x=1}^{M}\sum_{n_y=1}^{N} I_{m_x n_y} e^{j(n_y-1)(kd_y \sin\theta\sin\varphi+\beta_y)} e^{j(m_x-1)(kd_x \sin\theta\cos\varphi+\beta_x)} \quad (15)$$

The array response vector of the URPA is the product of the array response vectors of the ULAs in the x and y directions. The applied excitation amplitudes are set to $I_{m_x n_y} = 1$ and the progressive phase shifts in x and y directions are set to $\beta_x = 0^\circ$ and $\beta_y = 0^\circ$, respectively. The total number of antenna elements in the x and y directions are selected to be (M = 9) and (N = 14), respectively. The geometrical area for a URPA is $26\lambda_o^2$.

C. Uniform Circular Array (UCA)

The UCA can also be implemented to increase the gain. Fig. 3 shows the configuration of a circular array with radius (r) and the total number of equispaced elements N_r). The array response vector of the UCA is given as [22]

$$\mathbf{a}_r(\varphi,\theta)_{\text{UCA}} = \sum_{n_a=1}^{N_r} I_{n_a} e^{j\left(kr\sin\theta\cos(\varphi-\varphi_{n_a})+\beta_{n_a}\right)} \quad (16)$$

where the angular position of the n_a element is $\varphi_{n_a} = 2\pi n_a/N_r$. The excitation amplitudes are set to $I_{n_a} = 1$, and the phase excitation of the n_a element is set to $\beta_{n_a} = 0^\circ$. The diameter of a UCA is about $20\lambda_o$.

D. Uniform Circular Planar Array (UCPA)

The configuration of the UCPA is illustrated in Fig. 4. It consists of several circular rings with different radii $(r_{m_a n_a})$ and the same center. The antenna array elements are placed at equal distances on the circumference of each ring. The array response vector of the UCPA could be expressed as follows [22]

$$\mathbf{a}_r(\varphi,\theta)_{\text{UCPA}} = \sum_{m_a=1}^{M_m}\sum_{n_a=1}^{N_m} I_{m_a n_n} e^{j\left(kr_{m_a n_a}\sin\theta\cos(\varphi-\varphi_{m_a n_a})+\beta_{m_a n_a}\right)} \quad (17)$$

where $\varphi_{m_a n_a} = 2\pi n_a/N_m$ is the azimuth angle of n_a element in the m_a ring, respectively. The excitation weights are set to $I_{m_a n_n} = 1$ and the progressive phase shift of the n_a element in the m_a ring is set to $\beta_{m_a n_a} = 0^\circ$. For a UCPA, the total number of antenna elements on the m_a ring is $6m_a$, so the 126 antenna elements are distributed on 6 rings as ($N_1 = 6 : N_2 = 12 : N_3 = 18 : N_4 = 24 : N_5 = 30 : N_6 = 36$). The radius of each ring $r_{m_a n_n}$ is selected to provide $\lambda_o/2$ inter-element spacing at the angular direction. The geometrical area of the UCPA is about $25.8\lambda_o^2$.

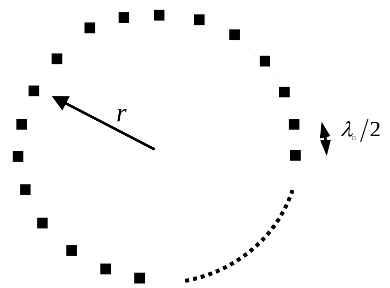

Fig. 3. The configuration of Uniform Circular Array (UCA).

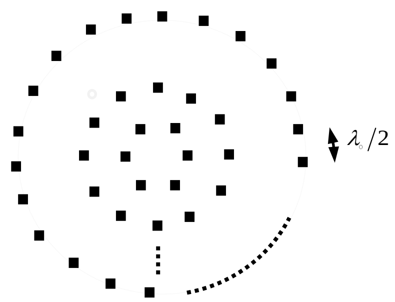

Fig. 4. The configuration of Uniform Circular Planar Array (UCPA).

VI. NUMERICAL RESULTS

In this section, the 2D directivity patterns for different antenna array configurations at the BS are simulated using MATLAB. Fig. 5 shows the 2D directivity patterns for the ULA, UCA, UCPA, and URPA antenna array configurations when each of these antenna arrays consists of 126 antenna elements and the azimuth angle is 0 degrees. The ULA at the BS has maximum and minimum directivity of 20.27 dBi and –77.74 dBi**,** respectively. The ULA at the BS has a null-to-null beam-width of 22°. The URPA at the BS provides a null-to-null beam-width of 30.92°, and it has maximum and minimum directivity of 22.68 dBi and –29.44dBi, respectively. The main beam of the URPA at the BS is wider due to the decrease in the aperture size. The UCA at the BS has maximum and minimum directivity of 21.14 dBi and –44.19 dBi**,** respectively; while its null-to-null beam-width is 6°. The UCA has a high angular resolution because of its large aperture size. The 2D maximum and minimum directivity for the UCPA at the BS are 22.68 dBi and –87.36 dBi, respectively. The null-to-null beam-width for the UCPA is 21.56°. The aperture size for the UCPA is small at the BS, so its angular resolution is decreased. The comparison between the antenna array configuration at the BS is indicated in Table II.

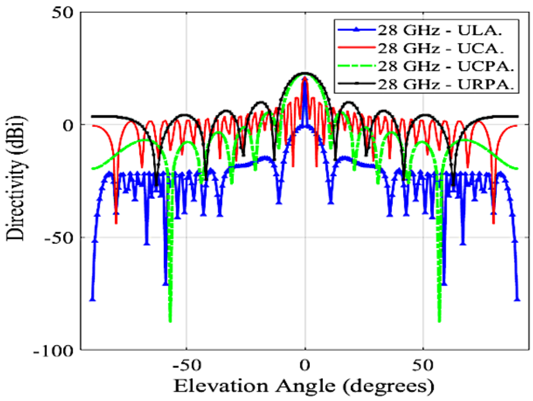

Fig. 5. 2D directivity patterns for different antenna array configurations at the BS (126 antenna elements, azimuth angle = 0 degrees).

TABLE II: COMPARISON BETWEEN THE ANTENNA ARRAY CONFIGURATIONS AT THE BS

Antenna array configuration at the BS	Maximum directivity for the 2D directivity pattern	Minimum directivity for the 2D directivity pattern	Difference between maximum and minimum directivity	Null-to-null beam-width
ULA	20.27 dBi	–77.74 dBi	98.01 dBi	22°
UCA	21.14 dBi	–44.19 dBi	65.33 dBi	6°
UCPA	22.63 dBi	–87.36 dBi	109.99 dBi	21.56°
URPA	22.63 dBi	–29.44 dBi	52.12 dBi	30.92°

The performance and the complexity of a detector based on exact MMSE and also iterative matrix inversion methods will be presented in bit error rate (BER) versus the signal to noise ratio (SNR). A comparison between the SOR, GS, RI, JA, and CG methods will be provided in different antenna array configurations, i.e., ULA, URPA, UCPA, and UCA. All simulations are carried out with the mmWave channel model introduced in (2) which has five clusters N_{cl}=5 and the number of rays within each cluster is ten N_{ray}=10. The modulation scheme is 16QAM, and 126×18 MIMO system. The impact of n and the computational complexity will be discussed as well. As given in (14) to (17), each antenna array configuration has its array response vector. The wireless channel matrix **H** is a function of the array response vector as given in (2) so that the wireless channel matrix is based on the antenna array configuration. The values of the elements of **H** will be varied when the antenna array configuration is changed and this will result in having a different value of the estimated signal and BER for each antenna array configuration as given in (6), (8) to (10), (12), and (13). Fig. 6 illustrates the BER performance of the MMSE detector in different antenna array configurations at the BS. It is clear that the URPA has achieved the best performance while the UCPA has the lowest BER. For instance, the BER=10^{-4} is achieved at SNR = 9dB, 11dB, 12dB, and 20dB in URPA, UCA, ULA, and UCPA, respectively. However, the MMSE-based detector is not desired in implementation because of a matrix inverse component. Therefore, iterative matrix inversion methods are applied. A better BER performance of the MMSE detector is obtained with the lower value of the difference between the maximum and the minimum directivity as illustrated in Table II.

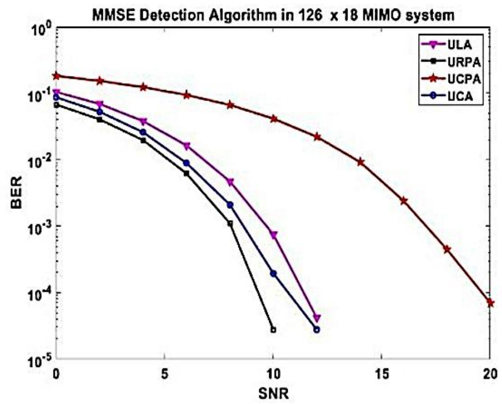

Fig. 6. Performance of MMSE detector in different antenna array configurations.

Fig. 7 shows the BER performance of the GS detector through different antenna array configurations at the BS and n=8. In this detector, the UCA has obtained the best performance while the URPA and UCPA had the worst. It is clear that the UCPA and URPA require more iterations to achieve satisfactory performance. The BER=10^{-4} is achieved at SNR = 12dB and 16dB in UCA, and ULA, respectively. Fig. 8 illustrates the BER performance of the SOR detector through different antenna array configurations at the BS, and at n=8. In this detector, the UCA has obtained the best performance while the URPA and UCPA had the worst. It is also clear that the UCPA and URPA require more iterations to achieve satisfactory performance. The BER=10^{-4} is achieved at SNR = 12dB and 14dB in UCA, and ULA, respectively. Fig. 9 illustrates the BER performance of the CG detector through different antenna array configurations at the BS, and at n=8. In this detector, the UCA has obtained the best performance while the URPA and UCPA had the worst. It is also clear that the UCPA and URPA require more iterations to achieve satisfactory performance. The BER=10^{-4} is achieved at SNR = 12dB and 14dB in UCA, and ULA, respectively.

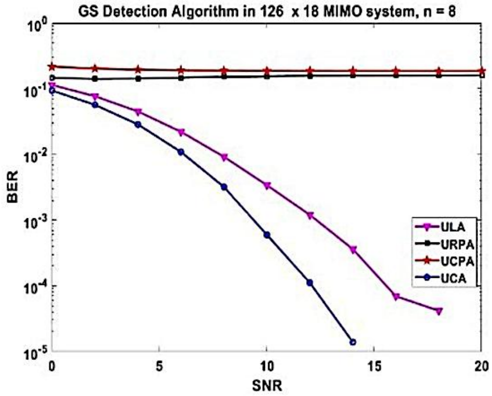

Fig. 7. Performance of the GS detector in different antenna array configurations.

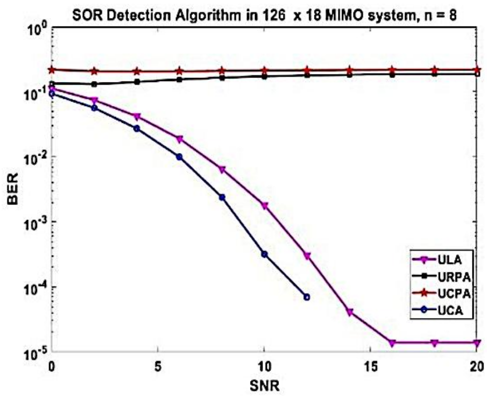

Fig. 8. Performance of the SOR detector in different antenna array configurations.

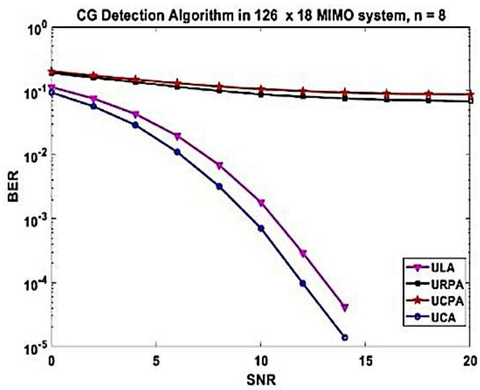

Fig. 9. Performance of the CG detector in different antenna array configurations.

Fig. 10 illustrates the BER performance of the JA detector through different antenna array configurations at the BS, and n=8. The JA detector is not applicable to the ULA, URPA, UCPA, and UCA. It has unsatisfactory performance over all iterations and antenna array configurations. Fig. 11 illustrates the BER performance of the RI detector through different antenna array configurations at the BS, and n=8. In this detector, the UCA has obtained the best performance while the URPA and UCPA had the worst. It is also clear that extra iterations are required to achieve the target BER=10^{-4}. As indicated in Table II, it is noted that the best BER performance with the SOR, GS, RI, and CG detection methods is achieved as the values of the null-to-null beam-width and the difference between the maximum and the minimum directivity are decreased. Fig. 12 to Fig. 15 illustrates the comparison among the proposed detectors over all types of antenna array configurations at the BS in terms of computational complexity. The detector based on the CG method has the lowest computational complexity while the RI method has the highest complexity. The SOR and the GS methods have a reasonable computational complexity. It is also noteworthy that the CG detector achieves the lowest computational complexity with satisfactory performance. A detector based on the JA method is not included in the complexity comparison chart because it is not robust in performance.

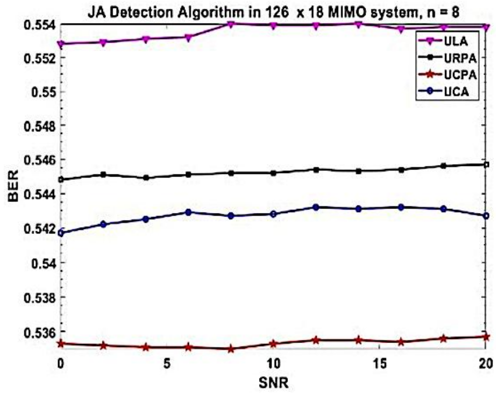

Fig. 10. Performance of the JA detector in different antenna array configurations.

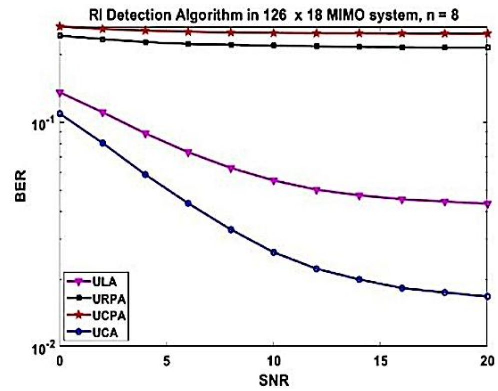

Fig. 11. Performance of the RI detector in different antenna

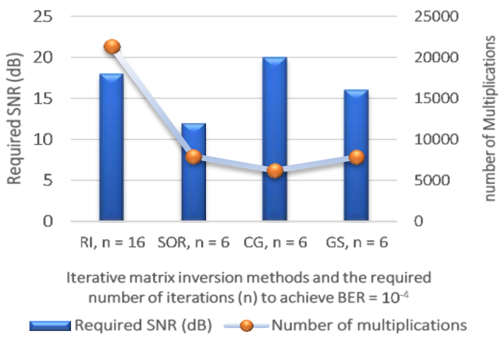

Fig. 12. A comparison between iterative matrix inversion methods to achieve the target BER when UCA is used.

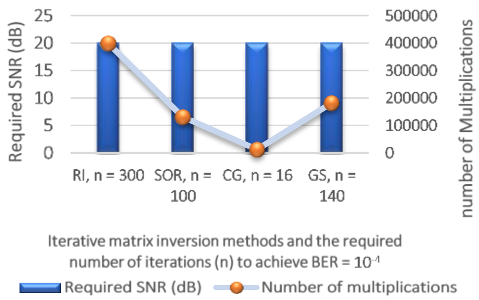

Fig. 13. A comparison between iterative matrix inversion methods to achieve the target BER when UCPA is used.

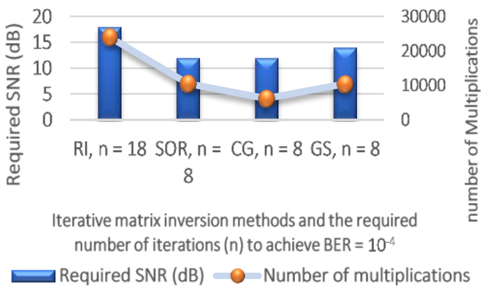

Fig. 14. A comparison between iterative matrix inversion methods to achieve the target BER when ULA is used.

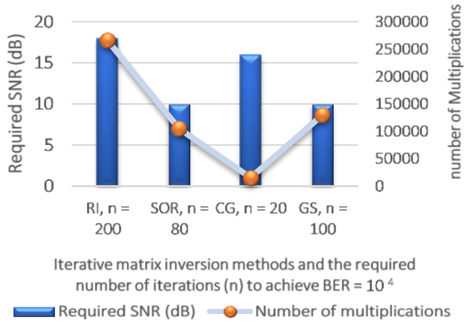

Fig. 15. A comparison between iterative matrix inversion methods to achieve the target BER when URPA is used.

VII. Discussion and Conclusion

This is the first paper to examine the effect of antenna array configurations at the BS on the performance and computational complexity of massive MIMO detection techniques. We investigated the performance of massive MIMO detection techniques with different antenna array configurations at the BS in the mmWave channel. The simulation results showed that the antenna array configuration at the BS can influence the performance of the massive MIMO detection techniques. We found that the implementation of URPA at the BS with the MMSE detection algorithm outperforms the other antenna array configurations. The deployment of UCA at the BS provides the best performance with the SOR, GS, RI, and CG detection methods. Although a detector based on JA method can be easily implemented, it is not applicable to the ULA, URPA, UCPA, and UCA due to a slow convergence rate, hence, implying a high latency. In addition, a comparison among detection techniques has been conducted in terms of computational complexity. The detector based on the CG method has the lowest computational complexity while the RI method has the highest complexity.

Conflict of Interest

The authors declare no conflict of interest.

Author Contributions

All authors conducted the research and analyzed the data. Author 1 wrote Sections II and V; author 2 wrote Sections III and IV; all authors wrote Sections I, VI, and VII; all authors had approved the final version.

References

[1] X. Yu, J. Shen, J. Zhang, *et al*., "Alternating minimization algorithms for hybrid precoding in millimeter wave MIMO systems," *IEEE Journal of Selected Topics in Signal Processing*, vol. 10, no. 3, pp. 485-500, 2016.

[2] F. B. Gross, *Smart Antennas with MATLAB*, 2nd ed. McGraw-Hill, 2015, ch. 4, pp. 90-105.

[3] N. Amani, A. Farsaei, U. Gustavsson, T. Eriksson, F. M. J. Willems, M. V. Ivashina, and R. Maaskant, "Array configuration effect on the spatial correlation of MU-MIMO channels in NLoS environments," in *Proc. 14th European Conf. on Antennas and Propagation*, 2020.

[4] W. Liu, Z. Wang, C. Sun, *et al*., "Structured non-uniformly spaced rectangular antenna array design for FD-MIMO systems," *IEEE Transactions on Wireless Communications*, vol. 16, no. 5, pp. 3252-3266, 2017.

[5] M. A. Albreem, M. Juntti, and S. Shahabuddin., "Massive MIMO detection techniques: A survey," *IEEE Communications Surveys & Tutorials*, vol. 21, no. 4, pp. 3109-3132, 2019.

[6] S. Yang and L. Hanzo., "Fifty years of MIMO detection: The road to large-scale MIMOs," *IEEE Communications Surveys & Tutorials*, vol. 17, no. 4, pp. 1941-1988, 2015.

[7] M. A. Albreem, W. Salah, A. Kumar, *et al*., "Low complexity linear detectors for massive MIMO: A comparative study," *IEEE Access*, vol. 9, pp. 45740-45753, Mar. 2021.

[8] M. Albreem, M. Juntti, and S. Shahabuddin, "Efficient initialisation of iterative linear massive MIMO detectors using a stair matrix," *Electronics Letters*, vol. 56, no. 1, pp. 50-52, 2020.

[9] M. Albreem, A. Alhabbash, A. Abu-Hudrouss, and T. Almohamad, "Data detection in decentralized and distributed massive MIMO networks," *Computer Communications*, vol. 189, pp 79-99, May 2022.

[10] W. Tan, X. Feng, G. Liu, W. Tan, *et al*., "Spectral efficiency of massive MIMO systems with multiple sub-arrays antenna," *IEEE Access*, vol. 6, pp. 31213-31223, June 2018.

[11] W. Tan, S. Jin, J. Wang, *et al*., "Achievable sum-rate analysis for massive MIMO systems with different array configurations," in *Proc. IEEE Wireless Communications and Networking Conference*, 2015, pp. 316-321.

[12] X. Wu, N. C. Beaulieu, and D. Liu, "On favorable propagation in massive MIMO systems and different antenna configurations," *IEEE Access*, vol. 5, pp. 5578-5593, Apr. 2017.

[13] Q. Ding, Y. Deng, X. Gao, and M. Liu, "Hybrid precoding for mmWave massive MIMO systems with different antenna arrays," *China Communications*, vol. 16, no. 10, pp. 45-55, 2019.

[14] A. Yu, J. Shusen, T. Xiaosi, *et al*., "Efficient successive over relaxation detectors for massive MIMO," *IEEE Trans. on Circuits and Systems I: Regular Papers*, vol. 67, no. 6, pp. 2128-2139, 2020.

[15] M. A. Albreem, "Approximate matrix inversion methods for massive MIMO detectors," in *Proc. IEEE 23rd International Symposium on Consumer Technologies*, 2019, pp. 87-92.

[16] Z. Xiaoqing, Z. Li, S. Xing, *et al*., "An improved Jacobi-based detector for massive MIMO systems," *Information*, vol. 10, no. 5, pp. 165–170, 2019.

[17] I. A. Khoso, D. Xiaoming, M. N. Irshad, *et al*., "A low-complexity data detection algorithm for massive MIMO systems," *IEEE Access*, vol. 7, pp. 39341-39351, Mar. 2019.

[18] M. A. Albreem, M. H. Alsharif, and S. Kim, "A low complexity near-optimal iterative linear detector for massive MIMO in realistic radio channels of 5G communication systems," *Entropy*, vol. 22, no. 4, pp. 388-398, 2020.

[19] B. Constantine, *Antenna Theory: Analysis and Design*, 4th ed. New Jersey, Canada: Wiley, 2016, ch. 6, pp. 285-368.

[20] R.-L. Haupt, *Antenna Arrays: A Computational Approach*, 1st ed. New Jersey, Canada: Wiley-IEEE Press, 2010, ch. 2, pp. 45-67.

[21] W. Tan, S. D. Assimonis, M. Matthaiou, *et al*., "Analysis of different planar antenna arrays for mmWave massive MIMO systems," in *Proc. IEEE 85th Vehicular Technology Conf.*, 2017.

[22] N. H. Noordin, V. Zuniga, A. O. El-Rayis, *et al*., "Uniform circular arrays for phased array antenna," in *Proc. Loughborough Antennas & Propagation Conf.*, Loughborough, 2011.

Mohamed Elhefnawy received a Ph.D. degree in communications engineering from USM University, Malaysia, in 2010. He is currently a Lecturer in the Department of Electrical Engineering at the Faculty of Engineering, October 6 University, Egypt. He has a strong academic background that includes: RF/ microwave engineering, electromagnetic theory, and antenna theory. In addition to his expertise in antenna design, he has a particular set of skills in Electromagnetic simulation tools such as ADS and CST, and simulation of systems using MATLAB and Simulink. He got the "Sanggar Sajung" Award for Excellence in Publishing, University of Science Malaysia (USM), 2009.

Mahmoud A. Albreem (Senior Member, IEEE) received the B.Eng. degree in electrical engineering from Islamic University of Gaza, Palestine, in 2008, and the M.Sc. (EE) and Ph.D. (EE) degrees from University Sains Malaysia (USM), Malaysia, in 2010 and 2013, respectively. From 2014 till 2016, Dr. Albreem was a Senior Lecturer with University Malaysia Perlis. In 2016-2021, he chaired Department of Electronics and Communications Engineering, A'Sharqiyah University, Oman. Currently, he is an Assistant Professor with Department of Electrical Engineering, University of Sharjah, UAE. He is also a Visiting Assistant Professor with Centre for Wireless Communications (CWC), University of Oulu, Finland. Dr. Albreem is the author of more than 70 journal and conference papers. He received several scholarships and grants, such as Nokia Foundation Centennial Grant (2018), USM Fellowship (2011-2013), and Best Master's Thesis Award of the School of Electrical and Electronics Engineering, USM (2010). Dr. Albreem served on the Editorial Board for Journal of Wireless Communications and Mobile Computing. His research interests include multiple-input multiple-output detection and precoding techniques, machine learning applications for wireless communication systems, and green communications.